Chemical Vapor Deposition of Iron and Iron Oxide Thin Films from Fe(II) Dihydride Complexes

Sungho Park, Sangho Lim, and Hyungsoo Choi*

Micro and Nanotechnology Laboratory and Department of Electrical and Computer Engineering, University of Illinois at Urbana−Champaign, Urbana, Illinois 61801

Received January 25, 2006
Revised Manuscript Received July 13, 2006

Iron oxides such as hematite (α-Fe_2O_3), maghemite (γ-Fe_2O_3), and magnetite (Fe_3O_4) are attractive materials due to their high catalytic activity in reducing hydrocarbons and magnetic and magneto-optical properties.[1−2] Currently, attention is focused on thin films and nanoparticles of the spinel-type iron oxides (i.e., γ-Fe_2O_3 and Fe_3O_4), because they exhibit higher coercivity and signal-to-noise ratio than their bulk phases.[3] Because the properties of iron oxide films are dependent on their chemical composition and morphology, it is important to produce these films with high phase purity and good surface morphology.[4−5] Various methods have been employed to grow iron oxide thin films.[6−11]

Chemical vapor deposition (CVD) offers a convenient and inexpensive method for depositing high-quality metal oxide thin films. The CVD of iron oxide thin films has been reported using precursors such as $[Fe(O^tBu)_3]_2$, $Fe(CO)_5$, and $Fe(C_5H_7O_2)_3$.[3,11−17] However, because of the metastability of the spinel-type iron oxides, the Fe_2O_3 films tend to be formed rather than the Fe_3O_4, unless the processing conditions were tightly controlled. Even then, the Fe_3O_4 films were obtained often as mixed phase.[16] In addition, the effect of the processing conditions, such as the O_2 feed and the substrate temperature, on the formation of the Fe_3O_4 phase was reported to vary with precursor. For instance, the $Fe(CO)_5$ precursor produced α-Fe_2O_3 in the presence of O_2 and Fe−Fe_3O_4 composite in the presence of CO_2, where $[Fe(O^tBu)_3]_2$ produced α-Fe_2O_3 and Fe_3O_4 at 400 and 450 °C, respectively, in the absence of O_2.[3,15]

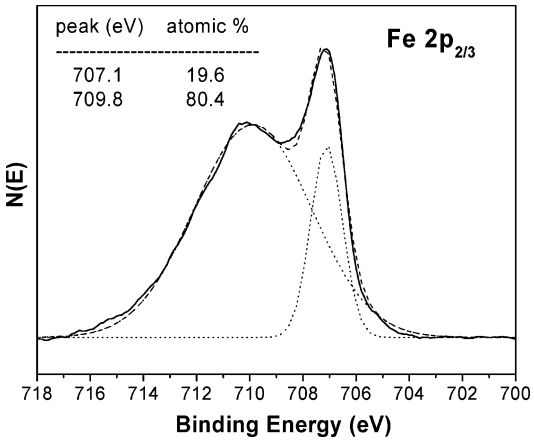

Figure 1. Fe $2p_{2/3}$ XPS spectrum of the Fe−Fe_3O_4 thin film deposited from $H_2Fe[P(OCH_3)_3]_4$.

Herein, we report the CVD of iron and iron oxide films using $H_2Fe[P(OCH_3)_3]_4$ and $H_2Fe[P(CH_3)_3]_4$ as precursors. $H_2Fe[P(OCH_3)_3]_4$ and $H_2Fe[P(CH_3)_3]_4$ were prepared according to the literature method by the reaction of $FeCl_2$ with $NaBH_4$ and the corresponding trimethylphosphite or trimethylphosphine.[18] CVD experiments were carried out in a cold-wall glass reactor with a bubbler-type precursor vessel maintained at 70−100 °C during the deposition process.[19] The precursor was injected into the reactor with argon as a carrier gas with flow rate of 200−300 sccm. A liquid nitrogen trap was connected to the reactor to collect any reaction byproducts. Oxygen gas was leaked into the reactor separately when needed. Film depositions were conducted on Si (111) substrates at 230 and 280 °C. The CVD chamber was evacuated to a background pressure of 1×10^{-6} Torr and maintained at 0.01−5 Torr during the deposition processes. The deposited films were analyzed by X-ray photoelectron spectroscopy (XPS), X-ray diffraction (XRD) method with Cu K_α radiation, and scanning electron microscopy (SEM). For the XPS analysis, the films were etched with argon ion for 5 min with a sputtering rate of 30 Å/min. The Scotch tape test indicated that the adhesion of the deposited films to the substrate was good.

No peaks were observed by XRD for the films deposited from $H_2Fe[P(OCH_3)_3]_4$ in the absence of any reactive gas such as H_2 or O_2 during the deposition process, indicating that the films were amorphous. The XPS spectra were obtained to analyze the composition of the deposited films. Figure 1 shows the Fe $2p_{2/3}$ core level XPS spectrum of the film grown from $H_2Fe[P(OCH_3)_3]_4$ at 280 °C. The peaks at 707.1 and 709.8 eV were consistent with the Fe $2p_{3/2}$ binding energies for Fe and Fe_3O_4, respectively, which suggested that

* Corresponding author. E-mail: hyungsoo@uiuc.edu.

(1) Vasiliev, A. A. *Sens. Actuators, B* **1992**, *7*, 626.
(2) Dimitrov, D. V.; Hadjipanayis, G. C.; Papaefthymiou, V.; Simopoulos, A. *IEEE Trans. Magn.* **1997**, *33*, 4363.
(3) Mathur, S.; Veith, M.; Sivakov, V.; Shen, H.; Huch, V.; Hartmann, U.; Gao, H. *Chem. Vap. Deposition* **2002**, *8*, 277.
(4) Izaki, M.; Shinoura, O. *Adv. Mater.* **2001**, *13*, 142.
(5) Pal, B.; Sharon, M. *Thin Solid Films* **2000**, *379*, 83.
(6) Ishii, Y.; Terada, A.; Ishii, O.; Ohta, S.; Hattori, S.; Makino, K. *IEEE Trans. Magn.* **1980**, *16*, 1114.
(7) Kim, Y. K.; Oliveria, M. *J. Appl. Phys.* **1993**, *75*, 431.
(8) Fujii, T.; Takano, M.; Katano, R.; Bande, Y. *J. Appl. Phys.* **1989**, *66*, 3168.
(9) Chen, M. M.; Oritz, C.; Lim, G.; Sigsbee, R.; Castillo, G. *IEEE Trans. Magn.* **1987**, *15*, 1549.
(10) Hattori, S.; Ishii, Y.; Shinohara, M.; Nakagawa, T. *IEEE Trans. Magn.* **1979**, *15*, 1549.
(11) Dhara, S.; Rastogi, A. C.; Das, B. K. *Thin Solid Films* **1994**, *239*, 240.
(12) Lie, M.; Fjellvåg, H.; Kjekshus, A. *Thin Solid Films* **2005**, *488*, 74.
(13) Marco de Ridder, M.; Van De Ven, P. C.; VanWelzenis, R. G.; Brongersma, H. H.; Helfensteyn, S.; Creemers, C.; Van Der Voort, P.; Baltes, M.; Mathieu, M.; Vansant, E. F. *J. Phys. Chem. B* **2002**, *106*, 13146.
(14) Yubero, F.; Ocaña, M.; Justo, A.; Contreras, L.; González-Elipe, A. R. *J. Vac. Sci. Technol., A* **2000**, *18*, 2244.
(15) Maruyama, T.; Shinyashiki, Y. *Thin Solid Films* **1998**, *333*, 203.
(16) Fujii, E.; Torii, H.; Tomozawa, A.; Takayama, R.; Hirao, T. *J. Cryst. Growth* **1995**, *151*, 134.
(17) Rastogi, A. C.; Dhara, S.; Das, B. K. *J. Electrochem. Soc.* **1995**, *142*, 3148.
(18) Gerlach, D. H.; Peet, W. G; Muetterties, E. L. *J. Am. Chem. Soc.* **1972**, *94*, 4545.
(19) Choi, H.; Park, S.; Jang, H. G. *J. Mater. Res.* **2002**, *17*, 267.

10.1021/cm0601990 CCC: $33.50
Published on Web 10/06/2006

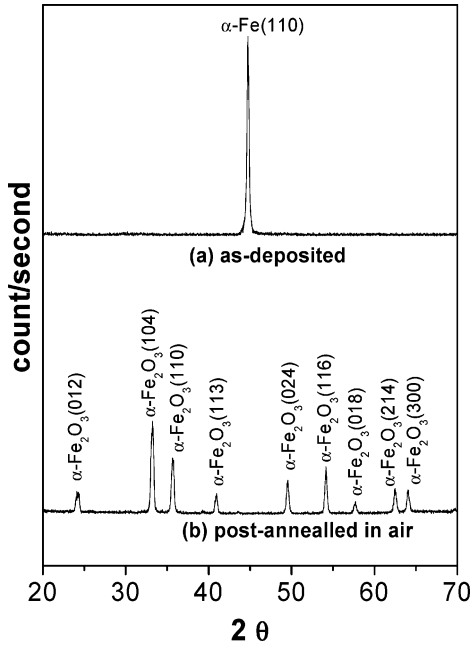

Figure 2. XRD patterns of the films grown from $H_2Fe[P(CH_3)_3]_4$: (a) as-deposited at 280 °C and (b) after annealing at 600 °C under air.

the film was an Fe−Fe_3O_4 composite with a ratio of 3:4.[20] Because no external oxygen source was provided, the oxygen in the film must have originated from the precursor molecule via the decomposition of the phosphite ligand, leading to the contamination of the deposited film. The incorporation of carbon was not detected by XPS; however, the incorporation of phosphorus in the film was ∼2 at %. The decomposition of the phosphite to produce Fe_3O_4 from $H_2Fe[P(OCH_3)_3]_4$ was rather intriguing considering the low substrate temperatures used in this study. In fact, although the M−O bond strength of cobalt or nickel is comparable to that of iron, both $HCo[P(OR)_3]_4$ and $Ni[P(OR)_3]_4$, where R = alkyl, produced highly pure cobalt and nickel film, respectively, liberating the phosphites intact under the same processing conditions.[21−23] If the decomposition of the phosphite involved dealkylation processes to afford a P═O bond, the low P content in the film was rather surprising. More detailed analysis of the deposited films is required to understand better the decomposition of the phosphite. The Fe−Fe_3O_4 composite was converted to α-Fe_2O_3 after annealing at 600 °C under air. In the presence of O_2, $H_2Fe[P(OCH_3)_3]_4$ produced amorphous Fe_2O_3 with a P contamination of ∼2 at % measured by XPS, indicating that the participation of the phosphite still took place. It is beyond the scope of the present work to discuss the detailed mechanism of the deposition process. However, the higher oxidation state of the iron than that of the cobalt or nickel in each precursor might have contributed to the iron oxide formation from $H_2Fe[P(OCH_3)_3]_4$ rather than iron metal in the absence of O_2 during the deposition process.

(20) *Handbook of X-ray Photoelectron Spectroscopy*; Wagner, C. D., Riggs, W. M., Davis, L. E., Moulder, J. F., Muilenger, G. E., Eds.; Perkin-Elmer: Eden Prairie, MN, 1979.
(21) Choi, H.; Park, S. *Chem. Mater.* **2003**, *15*, 3121.
(22) Choi, H.; Park, S.; Kim, T. H. *Chem. Mater.* **2003**, *15*, 3735.
(23) Pedley, J. B.; Marshall, E. M. *J. Phys. Chem. Ref. Data* **1983**, *12*, 967.

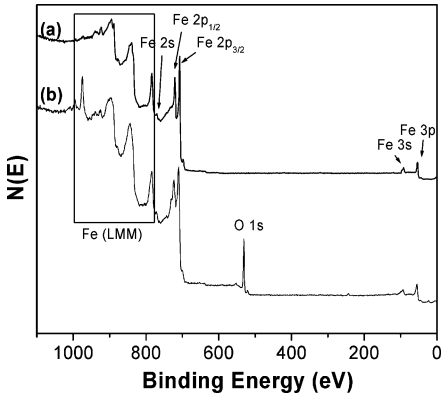

Figure 3. XPS spectra of the films deposited from $H_2Fe[P(CH_3)_3]_4$ at 280 °C: (a) without O_2 and (b) with O_2.

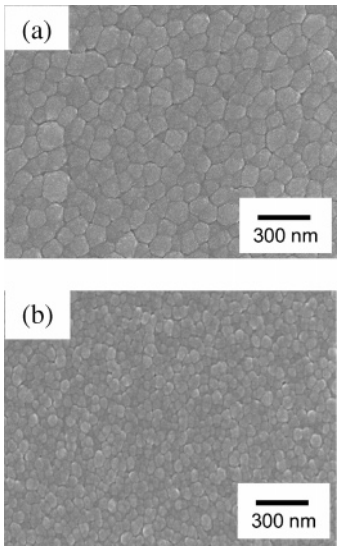

Figure 4. SEM images of α-Fe films deposited from $H_2Fe[P(CH_3)_3]_4$ at (a) 230 °C, and (b) 280 °C.

To rule out the effect of the intramolecular oxygen on the film formation during the CVD process, we employed $H_2Fe[P(CH_3)_3]_4$ as a precursor. The XRD pattern in Figure 2a indicates that the film deposited from $H_2Fe[P(CH_3)_3]_4$ at 280 °C was highly oriented α-Fe (110) phase with a cubic structure. Figure 3a shows an XPS spectrum of the film. The Fe $2p_{3/2}$ binding energy at 707.5 eV agrees well with that of the iron metal.[20] No C and P contaminants were detected in the film. ^1H NMR analysis indicated that the exhaust collected in the liquid nitrogen trap was the trimethylphosphine ligand liberated from the precursor molecule, which lends support to the high purity of the Fe film. Figure 4 shows the SEM images of the Fe films deposited at substrate temperatures of 230 and 280 °C. The grain sizes were about 120 nm for the film deposited at 230 °C and 50 nm at 280 °C. Grain size, in general, is expected to increase with temperature; however, the film deposited at 280 °C exhibited smaller grains. It seemed that the seed formation from $H_2Fe[P(CH_3)_3]_4$ was facilitated and prevailed over the grain growth at 280 °C. The α-Fe films were oxidized to α-Fe_2O_3 with a predominant rhombohedral structure after annealing at 600 °C under air. An XRD pattern of the film is shown in Figure 2(b).

In the presence of O_2, $H_2Fe[P(CH_3)_3]_4$ produced an iron oxide film. The XPS spectrum in Figure 3b shows binding

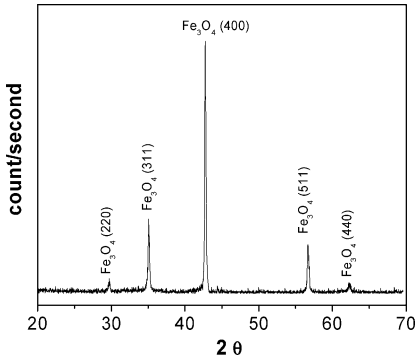

Figure 5. An XRD pattern of the Fe_3O_4 film deposited from $H_2Fe[P(CH_3)_3]_4$ at 280 °C.

Table 1. Properties of the Films Grown from $H_2Fe[P(OCH_3)_3]_4$ and $H_2Fe[P(CH_3)_3]_4$ at 280 °C.

	deposited film		
precursor	with O_2 feed	without O_2 feed	film properties[a]
$H_2Fe[P(OCH_3)_3]_4$	Fe_2O_3	Fe−Fe_3O_4	amorphous; P contamination
$H_2Fe[P(CH_3)_3]_4$	Fe_3O_4	α-Fe	crystalline; no detectable contamination

[a] Film properties were measured by XPS and XRD.

energy for O 1s and Fe $2p_{3/2}$ at 530.1 and 710.0 eV, respectively, indicating the film to be Fe_3O_4.[24−25] No C and P contaminants were detected in the film. The exhaust from the deposition reaction was analyzed by ^1H NMR to be trimethylphosphine dissociated from the precursor. The XRD pattern in Figure 5 indicated that the Fe_3O_4 film was polycrystalline. It was intriguing to observe that the phosphine ligand was dissociated from $H_2Fe[P(CH_3)_3]_4$ intact to produce pure and crystalline films, whereas the phosphite in $H_2Fe[P(OCH_3)_3]_4$ decomposed to give amorphous and contaminated films regardless of O_2 presence. Table 1 summarizes the properties of the films deposited from $H_2Fe[P(OCH_3)_3]_4$ and $H_2Fe[P(CH_3)_3]_4$. Squid measurements were performed on the Fe_3O_4 and Fe−Fe_3O_4 films deposited from $H_2Fe[P(CH_3)_3]_4$ and $H_2Fe[P(OCH_3)_3]_4$, respectively. Figure 6 presents the M−H characteristics of these films at room temperature. The crystalline Fe_3O_4 film exhibited

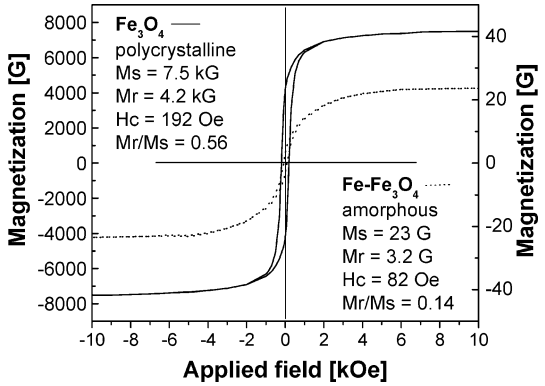

Figure 6. M−H characteristics for the Fe_3O_4 and Fe−Fe_3O_4 films.

higher values of saturation magnetization, remanent magnetization, and coercivity. The magnetic properties of the films deposited from the $H_2Fe[P(CH_3)_3]_4$ and $H_2Fe[P(OCH_3)_3]_4$ precursors regarding the crystallinity, microstructure, and purity are subjected to further study.

In summary, we have reported the CVD of Fe(II) dihydride complexes, $H_2Fe[P(CH_3)_3]_4$ and $H_2Fe[P(OCH_3)_3]_4$, to identify a viable precursor to grow iron and iron oxides. $H_2Fe[P(CH_3)_3]_4$ produced α-Fe films at substrate temperatures below 300 °C without employing H_2. With O_2 feed, the precursor deposited Fe_3O_4 films. Both films were crystalline and exhibited no detectable contamination by XPS. ^1H NMR analysis of the exhausts indicated that the phosphine ligand was liberated from the precursor molecule intact, supporting the high purity of the α-Fe and Fe_3O_4 films. On the other hand, $H_2Fe[P(OCH_3)_3]_4$ produced amorphous films containing impurities regardless of the O_2 presence, which indicated the decomposition of the phosphite ligand.

Acknowledgment. This work was partially supported by the National Science Foundation under Grant CHE-9973575. Park was supported by the Department of Defense Multidisciplinary University Research Initiative (MURI) program administered by the Office of Naval Research under Grant N00014-98-I-0604. The microanalysis contained in this work was carried out in the Center for Microanalysis of Materials, University of Illinois, which is partially supported by the U.S. Department of Energy under Grant DEFG02-96-ER45439.

CM0601990

(24) Schedel-Niedrig, T.; Weiss, W.; Schlögl, R. *Phys. Rev. B* **1995**, *52* (17), 449.
(25) Gao, Y.; Kim, Y. J.; Chambers, S. A. *J. Mater. Res.* **1998**, *13*, 2003.